Int. J. Heat Mass Transfer. Vol. 27, No. 1, pp. 57–67, 1984
Printed in Great Britain

0017 9310/84 $3.00 + 0.00

A FINITE ELEMENT ANALYSIS OF THE UPPER JET REGION OF A FIBER DRAWING FLOW FIELD OF A TEMPERATURE-SENSITIVE MATERIAL

RICHARD SAYLES* and BRUCE CASWELL
Division of Engineering at Brown University, Providence, RI 02912, U.S.A.

(*Received* 10 *August* 1982 *and in revised form* 4 *May* 1983)

Abstract—The finite element method was applied in an analysis of the convective cooling of the upper jet region of a fiber flow. This region is characterized by fully two-dimensional velocity and temperature fields, the appearance of a free surface, and a large attenuation of the jet radius. The convective heat transfer from the jet was calculated using a boundary layer theory in which the effect of the stretching jet surface is accounted for, and Reynolds' analogy was assumed for the calculation of convective heat transfer coefficients. Jet flows of an extremely temperature-sensitive material, Arochlor, were modeled. The free surface shapes of the jets, predicted with the finite element model, were compared to experimentally determined jet shapes. It was found that the degree of accuracy to which the free surface shape of a jet could be predicted using the finite element model was strongly dependent upon the amount of viscous dissipation present in the jet flow.

NOMENCLATURE

a	local jet radius
b_i	fluid body force vector
c_p	specific heat
F	viscous tension in the jet
h	trial function for pressure
k	thermal conductivity
$\dot{m}$	mass flow rate
n_i	unit vector normal to surface
Nu	Nusselt number
p	fluid pressure
q_i	heat flux vector
Q	volumetric flow rate
r, z	radial and axial coordinates
t_i	surface traction vector, $\sigma_{ij}n_j$
T	temperature
u, w	radial and axial velocity components
U_i	trial function for velocity
V_i	velocity vector
X_i	position vector.

Greek symbols

α	boundary layer parameter
γ	surface tension
δ_{ij}	Kronecker delta
θ	trial function for temperature
Θ	dimensionless temperature, $(T-T_\infty)/(T_0-T_\infty)$
μ, ν	absolute and kinematic viscosities
ρ	density
σ_{ij}	symmetric stress tensor
τ	shear stress
Φ	viscous dissipation.

Subscripts

a	air properties
m	mean—integrated across the flow field
0	initial conditions
s	conditions at the jet surface
∞	ambient conditions.

* Present address: Department of Mechanical Engineering, University of Maine, Orono, ME 04469, U.S.A.

INTRODUCTION

TYPICALLY, thin fibers are manufactured by forcing molten material through a nozzle or orifice into the atmosphere. The emerging jet cools by heat transfer to the environment, and after solidifying is wound up on a take-up roller. Regulation of the speed of the take-up roller gives rise to a tensile force at the end of the jet which causes the latter to be drawn out into a thin fiber.

A fiber drawing flow field can be divided into three distinct regions. The upper jet region is characterized by fully two-dimensional (2-D) fields and a large attenuation of the radius of the jet. Downstream from the upper jet region is the central jet region which is characterized by a uniform distribution of the axial velocity across the jet, and small slope of the free surface. Still farther downstream is the constant radius region where no further attenuation of the jet occurs.

In the central and lower portions of the jet, the slope can be used as a small parameter to simplify the governing equations. The resulting ordinary differential equations constitute the small slope theory as derived by Glicksman [1]. The complexities of the upper jet region point to numerical methods of solution. The abrupt changes in boundary conditions together with the appearance of a free surface are complexities particularly suited to the finite element method.

In the process of drawing glass fibers, the initial melt temperature could reach 1200–1500°C. At these initial temperatures, radiation heat transfer is predominant. As a glass jet is drawn through the atmosphere, it experiences an extreme change in temperature resulting in large variations in viscosity. To determine the shape of a jet which undergoes large changes in viscosity during its formation, one must accurately

predict the heat transfer from the jet to the surroundings. At some point in the cooling process, convective heat transfer becomes important. Before considering problems in which all of the modes of heat transfer occur simultaneously, it is constructive to examine the convective mode independently. This paper deals with materials which can be drawn at low temperatures and also exhibit temperature-sensitivity of flow properties. A chlorinated aromatic hydrocarbon, Arochlor, was used by Krishnan [2] in experiments on fiber drawing at about 60°C, at which temperature radiation effects are much smaller than forced convection heat transfer. Krishnan measured the flow properties of Arochlor necessary for the analysis of the jet flow. His data show that Arochlor undergoes extreme variations in viscosity for relatively small temperature changes, and for this reason it is a unique example of a temperature-sensitive material. Because of its strongly temperature-dependent viscosity, Arochlor may be considered to be the low temperature analog of glass. That is, without the complexity of radiation heat transfer, it is possible to study, at low temperatures, flows characterized by large viscosity changes similar to those occurring in glass at high temperatures.

In an earlier work [3] it was shown that the development of the laminar viscous boundary layer on an attenuating jet may differ significantly from that which is normally associated with a rigid surface [4]. If Reynolds' analogy is assumed for the calculation of convective heat transfer to an air atmosphere, it was found that the effect of the stretching jet was to increase the calculated heat transfer rate and, consequently, the jet will attenuate less if its viscosity is temperature-dependent.

THE FINITE ELEMENT EQUATIONS AND THE AXFIN COMPUTER PROGRAM

The conservation equations for mass, momentum, and energy for the flow of an incompressible, Newtonian fluid are

$$\frac{\partial V_j}{\partial x_j} = 0, \tag{1}$$

$$\rho V_j \frac{\partial V_i}{\partial x_j} = \rho b_i + \frac{\partial \sigma_{ij}}{\partial x_j}, \tag{2}$$

and

$$\rho c_p V_j \frac{\partial T}{\partial x_j} = \sigma_{ij} \frac{\partial V_i}{\partial x_j} - \frac{\partial q_j}{\partial x_j}, \tag{3}$$

where

$$q_j = -k \frac{\partial T}{\partial x_j},$$

and

$$\sigma_{ij} = -p\delta_{ij} + \mu\left(\frac{\partial V_i}{\partial x_j} + \frac{\partial V_j}{\partial x_i}\right).$$

The usual summation convention is assumed for repeated indices in the above equations.

A finite element computer program called AXFIN has been developed to solve the conservation equations. In the AXFIN program, the conservation equations are solved by the method of weighted residuals [5], and Galerkin's criteria is invoked to require the respective residuals of mass, momentum, and energy to vanish over the solution domain. Therefore, Galerkin statements of the conservation equations, in which velocity, pressure, and temperature have been chosen to be the independent field variables, are

$$\int_v \left[\rho V_j \frac{\partial V_i}{\partial x_j} U_i + \sigma_{ij} \frac{\partial U_i}{\partial x_j} - \frac{\partial V_j}{\partial x_j} h\right] \mathrm{d}v = \int_v \rho b_i U_i \, \mathrm{d}v + \int_S t_i U_i \, \mathrm{d}S, \tag{4}$$

for $i = 1$, 2, and 3, and

$$\int_v \left[\rho c_p V_j \frac{\partial T}{\partial x_j} \theta - q_j \frac{\partial \theta}{\partial x_j}\right] \mathrm{d}v = \int_v \sigma_{ij} \frac{\partial V_i}{\partial x_j} \theta \, \mathrm{d}v - \int_S q_i n_i \theta \, \mathrm{d}S. \tag{5}$$

The incompressibility constraint has been invoked in the third term of equation (4). This finite element formulation of the conservation equations has been widely used and accepted by workers in this field [6, 7], and needs no further explanation.

This paper is concerned with axisymmetric, steady flows which have been solved with a modified version of the AXFIN computer program. The isothermal version of AXFIN is described in ref. [8], and its extension to non-isothermal flows [9] incorporates a non-symmetric equation solver required for the treatment of the convective terms in the momentum and energy equations. Triangular elements are used in which the velocity components and the temperature are interpolated at each corner and midside of the triangles (quadratic interpolation). The pressure is interpolated only at the corners of the triangles (linear interpolation). For flow problems with axisymmetric geometries, the volume integrations specified in equations (4) and (5) reduce to area integrals, and the surface integrations reduce to line integrals around the solution domain. In the AXFIN program the area integrations are performed by a seven-point Gaussian quadrature.* For problems in which the fluid mechanics and energy equations are coupled through temperature-dependent viscosity, an alternating solution technique is employed. Successive velocity and temperature fields are calculated until a suitably converged solution is obtained.

* The algebraically exact area integrations described in ref. [12] are not used in this work.

MODELING THE UPPER JET REGION OF A FIBER FLOW

The upper jet region of a fiber flow field is that region in which the velocity field changes from a fully 2-D field at the nozzle exit to a one-dimensional (1-D) distribution, which occurs typically between two and six radii downstream from the nozzle exit.

The following is proposed as a model of a jet flow. The hot melt is assumed to emerge from a long circular tube into a still isothermal atmosphere where it cools until solidifying; it is then wound up on a take-up roller. It is neither necessary nor practical to consider the complete length of the jet for the finite element analysis. The region of interest is the first seven or eight tube radii of the flow field downstream from the exit. From Fig. 1 it is clear that two cuts must be made across the flow field. Since the governing equations are elliptic in character, one must have an accurate knowledge of the local flow conditions at these locations such that the boundary conditions needed to solve the problem are known. If a judicious choice is made for the location of the cuts through the flow field, a minimum disturbance will result in the numerical solution. The first cut is made across the internal pipe flow field far enough upstream from the exit such that fully developed Poiseuille flow exists. This cut should be made at least two radii upstream from the pipe exit plane. The second cut through the flow field is made at a point far enough downstream from the pipe exit such that the theory of small slopes, to be discussed below is applicable. The point at which the small slope theory becomes applicable has been found to be typically two to three radii downstream from the pipe exit for isothermal jets [10, 11], and four to five radii for jet flows with significant thermal coupling [12].

The flow domain used in this finite element analysis of jet flows may be summarized as follows (see Fig. 1): since the flow field is axisymmetric, the centerline of the jet is chosen as one boundary of the domain. The upstream cut through the flow field is made at a distance of four radii upstream from the pipe exit, and the downstream cut is made at a distance of eight radii downstream from the exit. As the hot fluid emerges from the pipe, the outer surface of the jet is a free surface in contact with the surrounding atmosphere. This free surface is subject to surface tension and air drag forces, and across it takes place the convection cooling of the jet. This flow domain corresponds to the physical dimensions of the jet flow fields reported in the experiments performed by Krishnan [2].

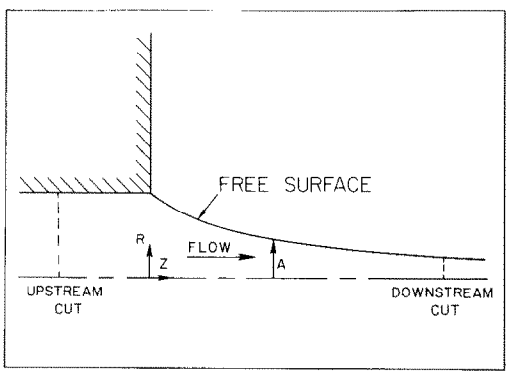

FIG. 1. The flow domain for analyzing the upper jet region of a fiber flow.

The shape of the free surface of the jet is computed by a numerical iteration scheme. An initial shape for the free surface of the jet is assumed which, usually, is a cylinder of constant radius. Then, with the appropriate boundary conditions applied to the flow domain, a velocity field is calculated. A new estimate for the shape of the jet is obtained from the calculated velocity field subject to the condition that the free surface of the jet is a streamline of the flow field. This iteration procedure is repeated until a suitably converged shape of the jet is obtained. The iteration scheme usually requires five or six iterations for an isothermal jet flow, and anywhere from 20 to 50 iterations for a jet flow with significant thermal coupling such as temperature-dependent viscosity.

The boundary conditions applied to the flow domain are now summarized. On the centerline of the jet: the radial velocity, the shear stress, and the radial heat flux are zero. On the upstream cut through the flow field: the radial velocity is zero, the axial velocity is assumed to be the fully developed Poiseuille flow distribution, and the jet fluid enters the flow domain with constant temperature. On the internal pipe surface: the no-slip condition is imposed, and zero normal heat flux is specified. On the free surface, surface tension forces are applied. If the ratio of the viscosity of air to the viscosity of the jet fluid is very small, the viscous shear stresses in the boundary layer on the jet will transmit negligible shear stress across the free surface into the jet flow. This will be the case for jets of highly viscous materials. However, if very long jets were considered, the total integrated air drag on the surface could be comparable to the drawing tension applied to the end of the fiber at the take-up roller.* Here air drag is neglected since only the first eight radii of the flow field downstream from the orifice exit are considered, and the jet fluid is highly viscous. The forced convection heat transfer from the free surface is calculated from a boundary layer theory to be described below. On the downstream cut through the flow field, viscous stresses and the heat flux are specified. The boundary conditions applied across the downstream cut are obtained from the small slope theory.

The isothermal small slope theory incorporates three basic assumptions: the axial velocity is uniform across the jet (w is independent of r), the local surface slope is small ($da/dz \ll 1$, hence, the name small slope theory), and negligible shear stress is transmitted from the air boundary layer into the jet. A detailed discussion of the

* Ben-Sabar [12] estimated the air drag on typical glass fibers to be about 40% of the drawing tension.

small slope theory is not necessary here since the theory is needed only to deduce the boundary conditions to be applied to the end of the jet. A detailed discussion of the small slope theory is given by Glicksman [1].

The stress boundary conditions applied to the end of the jet are obtained from the small slope theory. The normal stress component on a plane normal to the jet flow is

$$\sigma_{zz} = 3\mu \frac{dw}{dz}. \tag{6}$$

This expression for the normal stress is valid only in that region of the flow field where the small slope theory assumptions are applicable. In the above expression the total derivative of the axial velocity is used since it has been assumed that the axial velocity is uniform across the jet. This is consistent with the small slope theory assumption that there is negligible shear stress present in the jet flow. If the axial strain rate in the jet is independent of r and the viscosity of the fluid is constant, then the normal stress distribution on the end cut is uniform. This will be the case if the jet flow is isothermal, or the viscosity is independent of temperature. In a nonisothermal jet flow, the temperature field becomes fully two-dimensional; therefore, when the viscosity of the jet fluid is temperature-dependent, the normal stress on the end cut will not be uniform. In a shear flow a non-uniform distribution of viscosity across the flow field would modify the shape of the velocity profile. However, since the shear stress is negligible in the small slope region of the jet flows to be examined, the small slope theory conclusion that the axial strain rate in the jet is independent of r will not change even with large variations in the viscosity of the jet fluid across the flow field.* Therefore, the normal stress at any point on the cross-sectional plane normal to the jet flow is proportional to the local viscosity of the jet fluid multiplied by the axial strain rate. Typical normal stresses calculated from finite element solutions are in excellent agreement with the assumed distribution for normal stresses.

The heat flux boundary condition for the end of the jet is obtained from an approximate 1-D form of the energy equation consistent with the small slope theory. As previously mentioned, the temperature field in the jet never approaches a uniform distribution as the axial velocity field does. However, a 1-D approximate form of the energy equation may be obtained if the temperature field in the jet is integrated over a cross-section. This results in an ordinary differential equation for the mixed mean temperature, T_m

$$\rho c_p w \frac{dT_m}{dz} = \frac{2k}{a} \frac{\partial T}{\partial r}\bigg|_{r=a} + k \frac{d^2 T_m}{dz^2} + \Phi. \tag{7}$$

For a typical location of the downstream cut, the final jet radius is 10–50 times smaller than the tube radius. From equation (7), the axial conduction term, which is proportional to the local radius of the jet squared, becomes increasingly smaller as the jet attenuates. Therefore, if the axial conduction term in equation (7) is neglected, an approximation for the axial derivative of the mixed mean temperature is obtained from the remaining terms in the equation, and this furnishes the axial heat flux to be imposed across the end cut. The applicability of dT_m/dz for the estimation of the local heat flux depends on the fact that, although the temperature varies considerably in the radial direction, the temperature profiles do not change rapidly in the axial direction.

CONVECTIVE HEAT TRANSFER FROM A STRETCHING JET

For temperature-sensitive materials, the prediction of the free surface shape of the jet will be strongly affected by the estimation of convective heat transfer. Ben-Sabar [12] calculated the viscous air drag using a laminar boundary layer theory in which the radius of the jet was assumed to be constant (rigid cylinder theory), and he assumed Reynolds' analogy for the calculation of convective heat transfer coefficients. In the analysis of the boundary layer, the assumption that the radius of the jet is constant implies that at any axial location the boundary layer on the jet has developed from the orifice exit to this axial location as it would on a rigid cylinder with this local radius and local surface velocity; hence, the name rigid cylinder theory. Since the upper jet region undergoes a large attenuation of the jet radius, a boundary layer theory which assumes a constant radius is inadequate, and may lead to considerable error in the calculated heat transfer coefficients. A boundary layer theory which includes the effect of the stretching jet surface is used in this work. The equations for the air boundary layer on the jet are

$$\frac{\partial}{\partial r}(ru) + \frac{\partial}{\partial z}(rw) = 0, \tag{8}$$

$$\rho_a \left[u \frac{\partial w}{\partial r} + w \frac{\partial w}{\partial z} \right] = \frac{\mu_a}{r} \frac{\partial}{\partial r} \left(r \frac{\partial w}{\partial r} \right). \tag{9}$$

For the analysis of the boundary layer on a stretching fiber, the Karman–Pohlhausen momentum–integral method is used. Manipulating equations (8) and (9), and integrating the resulting equation through the boundary layer, one obtains the appropriate momentum–integral equation for the laminar boundary layer on a stretching fiber, which is

$$\frac{d}{dz} \int_a^\infty r w^2 \, dr = -\frac{a\tau_s}{\rho_a}. \tag{10}$$

A suitable velocity profile for the boundary layer flow field must be chosen. Here the following velocity profile is assumed

$$w = w_s \left[1 - \frac{1}{\alpha} \ln \left(\frac{r}{a} \right) \right]. \tag{11}$$

* This statement can be shown to be rigorously true, see for example ref. [13].

This form of the boundary layer velocity profile has been incorporated in many momentum–integral analyses of laminar boundary layers on long cylinders [4, 14–18]. This profile is motivated by the shearing flow between two concentric cylinders in relative axial motion with no applied axial pressure gradient. The result obtained when equation (11) is substituted into equation (10) is

$$[e^{2\alpha}(\alpha-1)+\alpha+1]\frac{d\alpha}{dz}$$

$$=\frac{2\pi v_a}{Q}\alpha^2-\frac{1}{2w_s}\frac{dw_s}{dz}[\alpha\, e^{2\alpha}-\alpha(2\alpha^2+2\alpha+1)]. \quad (12)$$

This equation was first derived by Moore and Pearson [18]. The second term on the RHS of this equation is present due to the stretching jet surface. A stretching jet imposes on the boundary layer a development which is distinct from that which is normally encountered on a constant radius cylinder.

The integration of equation (12) requires an initial value of $\alpha(z)$. The forced convection boundary layer originates at the orifice exit. Sakiadis [4] solved the problem of the laminar viscous boundary layer on a continuous constant radius cylinder which is emerging from a wall. His result for the initial development of the boundary layer is

$$\alpha = 2.25(v_a z/wa^2)^{1/2}. \quad (13)$$

With this result, equation (12) may be integrated numerically in the streamwise direction.

If Reynolds' analogy is assumed for the calculations of heat transfer from the surface of the jet to an air boundary layer, the local Nusselt number is

$$Nu = 1/\alpha. \quad (14)$$

Therefore, the forced convection heat transfer coefficients may be obtained by numerical integration of equation (12) in the streamwise direction.

The use of Reynolds' analogy for the estimation of heat transfer coefficients is a device which allows the influence of stretching on the temperature field of the jet to be studied. The breakdown of Reynolds' analogy is not just a matter of the Prandtl number not being equal to one. It is also necessary to account for the development of the surface temperature; this may be more important than the Prandtl number effect in the breakdown of Reynolds' analogy. The effect on the heat transfer coefficients of the developing surface temperature has not been studied and, therefore, cannot be accounted for in this analysis. However, the effect of the Prandtl number has been calculated by Bourne and Elliston [14], and based on their work the Nusselt numbers calculated here are over-estimated by about 10% for the flows examined.

The hot jet entering the cold surroundings will possibly give rise to free convection effects. Whereas the forced convection boundary layer originates at the orifice exit, the free convection boundary layer originates at some point far downstream from the orifice exit. The free convection flow is such that it will increase the effective velocity of the airflow relative to the moving fiber and thus increase the heat transfer from the fiber to the surroundings. The relative importance of free convection to forced convection depends on the ratio $Gr^{1/2}/Re$, where Gr is the Grashof number and Re is the Reynolds number. When Gr and Re are of the same order of magnitude, the boundary layer on the fiber is a fully mixed free and forced convection flow. The combined heat transfer effect of a mixed free and forced convection boundary layer flow is not simply additive. Sparrow *et al.* [19] found that the maximum increase in heat transfer in a combined free and forced convection boundary layer flow was 23% when the ratio $Gr^{1/2}/Re = 1.3$. However, this result is for mixed free and forced convection boundary layers which originate at the same location. Barnett [20] pointed out that comparative values of Gr and Re cannot be used in a fiber drawing flow since the free and forced convection boundary layers have different places of origin. Since there is no known way of dealing with this combined free and forced convection boundary layer problem in an analytic fashion, some assumptions have to be made. Barnett, in an analysis of very long drawn fibers, assumed total convective heat transfer coefficients which were the sum of a forced convection heat transfer coefficient, derived from the results of Sakiadis [4], and an additional 20% of an estimated free convection heat transfer coefficient. This analysis concerns the upper jet region which is near the orifice exit. The external orifice surface will impede the motion of a free convection airflow moving up the fiber, thus reducing the effect free convection has on the total heat transfer coefficient. Therefore, in the upper jet region, forced convection heat transfer should be predominent with free convection increasing the forced heat transfer coefficients by 5–10%. Assuming Reynolds' analogy results in a 10% over-estimation of the forced convection heat transfer coefficients, and free convection heat transfer effects result in a probable 5–10% under-estimation of the heat transfer coefficients. Hence, for this analysis, it is assumed that these two effects tend to cancel one another, and the total convection heat transfer coefficients are assumed to be those calculated from the boundary layer theory presented above with no correction factor applied.

RESULTS

The flows examined here are those reported in the experiments of Krishnan [2] who performed extrusion experiments for the purpose of comparing experimentally determined shapes of jets to those predicted by an analytic method. He experimented with Arochlor, a material which flows and can be drawn into a thin fiber at 60°C. At this moderate temperature convective heat transfer is the dominant mode.

In his paper, Krishnan commented that Arochlor could be drawn into a continuous fiber only over a very small range of orifice exit temperatures, although he did

Table 1. The material properties of Arochlor and the flow conditions of the experiments of Krishnan [2]*

Experiment	Flow conditions P1	P2
$\dot{m}$ (g min^{-1})	0.42	0.38
T_0 (°C)	62.22	64.44
T_0 (°C)	25.6	23.3
w_0 (cm s^{-1})	0.0721	0.0653
a_0 (cm)	0.134	0.134
a_f (cm)	0.0082	0.0148
μ_0 (P)	98 065	42 778

* Arochlor material properties: $c_p = 0.22$ cal g^{-1} °C^{-1}; $k = 0.00165$ cal s^{-1} cm^{-1} °C^{-1}; $\gamma = 60$ dyn cm^{-1}; $\rho = 1.72$ g cm^{-3}; $\mu = \exp[34.745 - 0.3737T]$, where T is in °C.

not specify the range of temperatures. He also commented that when too high a drawing tension was applied, the fibers broke during the drawing process. Consequently, Krishnan was able to obtain only two sets of data for the drawn Arochlor jets. The flow conditions of these jets have been used in the finite element analysis to compare the predicted shapes to those reported in the experimental results. The flow conditions of the experiments are listed in Table 1 along with the material properties of Arochlor.

The finite element grid used in this analysis is shown in Fig. 2(b). Quadrilateral elements are shown, each of which is further subdivided into four triangular elements within the AXFIN computer program. For the grid shown, there are 492 triangular elements with a total of 3454 degrees of freedom in the system. In the upstream region of the flow domain, there are five elements across the flow field. Due to the large attenuation of the jet radius, this is reduced to three elements across the flow field as the downstream cut is approached. At the tube exit there is a stress singularity and, therefore, a refined grid is used in this region.

A finite element analysis was performed for the flow conditions of Krishnan's experiment P2. The tension applied to the end of the jet was adjusted until a converged shape of the free surface was found, and the radius at the end of the jet from the finite element solution matched that reported in the experimental results. Krishnan was unable to measure the tension on these jets since Arochlor remains a sticky fluid at the temperatures of the experiments, and techniques available at that time required a truly solid zone to obtain a force measurement. It should be appreciated that the tension is not a free parameter, even though it is treated as such in these computations. Figures 2(a) and 3(b) are contour plots of the streamlines and isotherms in the jet from the finite element solution, respectively. For experiment P2, the radius at the end of the jet is 11% of the initial tube radius. Figure 4 shows the shape of the jet predicted by the finite element method compared to the experimental result. The curve labeled 'complete solution' represents a complete thermal analysis of this flow problem. That is, the energy equation includes the effects of convection, conduction, and viscous dissipation, and is coupled with the momentum equation through the temperature-dependent viscosity of the fluid. The tensile force needed to draw the jet down to the desired radius was found to be $F = 4114$ dyn. In Fig. 4, the curve labeled 'no dissipation' is a finite element solution with viscous dissipation effects neglected in the thermal analysis of this problem, and the curve labeled 'constant viscosity' is a finite element solution with no energy analysis of the problem. For the constant viscosity case, the viscosity is taken to be that based on the upstream temperature. The same tensile force ($F = 4114$ dyn) was applied to the ends of the jets for all three cases presented in Fig. 4. These three solutions show how various thermal effects influence the predicted shape of a jet. For these flow conditions, the viscous dissipation has a moderate effect on the predicted shape of the jet. The end radius from the solution omitting viscous dissipation is 36% larger than that from the complete thermal analysis solution. The significant thermal effect is the temperature-dependent viscosity. The end radius from the constant viscosity

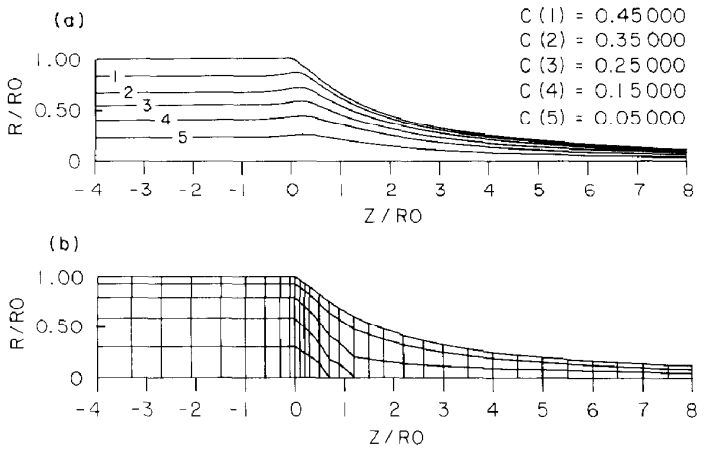

FIG. 2. (a) Streamlines from the finite element modeling of Krishnan's flow P2. (b) The finite element grid.

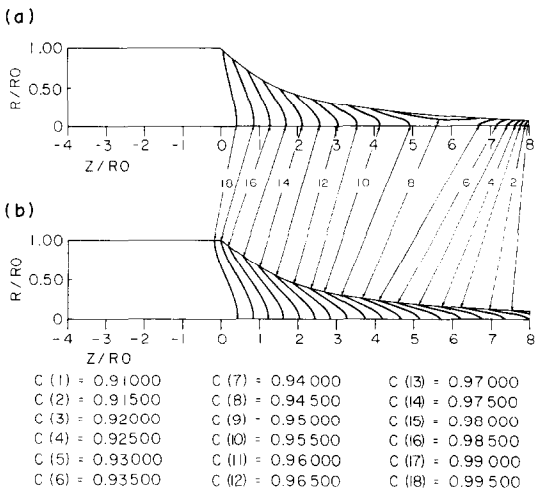

FIG. 3. (a) Temperature field from the finite element modeling of Krishnan's flow P1. (b) Temperature field from the finite element modeling of Krishnan's flow P2.

solution is 84% smaller than that from the complete thermal analysis solution.

Figure 5 compares the distribution of normal stress applied as boundary conditions to the end cut to that derived from the primitive variables of the finite element analysis of experiment P2. The stresses calculated from the finite element solution deviate by less than 1% from those applied to the end of the jet. The assumption that the axial strain rate in the jet is independent of r in the 1-D flow region, even in the presence of a fully 2-D temperature field, appears to be confirmed. Also, from the finite element solution, the radial distribution of the axial velocity is very uniform with a 0.03% deviation across the end cut, and a 4.0% deviation across the flow field four radii downstream from the tube exit.

In a previous work [3] the development of the viscous boundary layer on an attenuating jet was shown to be distinct from that which is normally encountered on a constant radius cylinder. The convective heat transfer from the jet to the surroundings is predicted to increase due to the

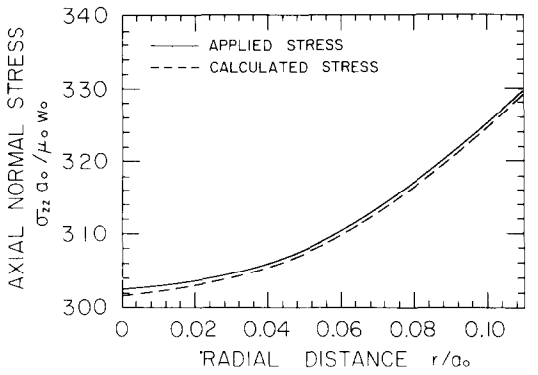

FIG. 5. Comparison of the normal stress applied to the end of the jet to that calculated from the finite element solution.

stretching effect, and this means that for fluids with temperature-dependent viscosity the predicted shapes of their jets will be modified. This effect can be shown by the following example. Consider two jets drawn with the same tension applied to the ends. For one jet, the stretching term is included in the boundary layer equation while for the second jet, the stretching term is omitted. The second case corresponds to applying the rigid cylinder boundary layer theory. The flow conditions imposed are those from Krishnan's experiment P2, and the drawing force applied to the ends of the jets is $F = 4114$ dyn. Figures 6–8 show the results of this comparison. Surface Nusselt number distributions calculated from the boundary layer equation (12) with and without the stretching term are presented in Fig. 6. Since the effect of stretching is to increase the Nusselt number, the thermal history of the jet is altered as seen in the plot of the mixed mean temperatures, Fig. 7. Also, since omission of the stretching effect reduces the heat transfer rate from the jet, the jet attenuates more as seen in Fig. 8. The difference in the end radii of the two jets was thus found to be 21%.

It is informative to compare the Nusselt numbers shown in Fig. 6 to those calculated from the empirical formula of Kase and Matsuo [21], $Nu = 0.265\,Re^{0.334}$ where the Nusselt number, Nu, and the Reynolds'

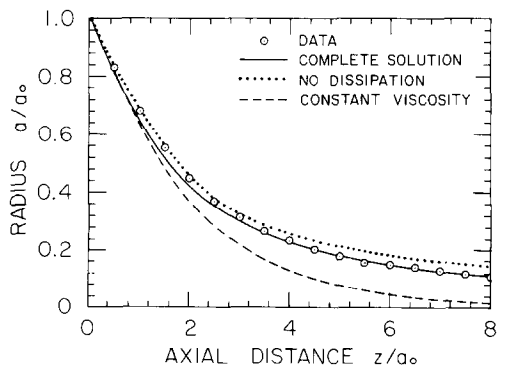

FIG. 4. Free surface shapes from the finite element solutions compared to Krishnan's data for the flow P2.

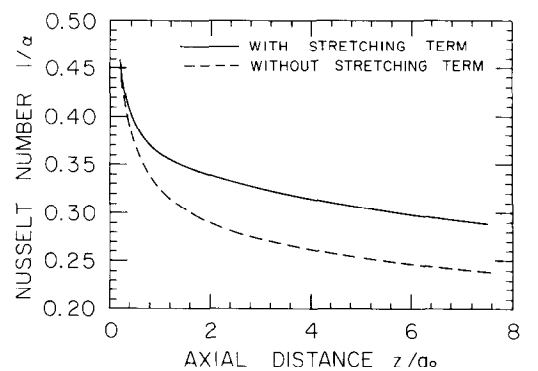

FIG. 6. Influence of stretching on the calculated Nusselt numbers.

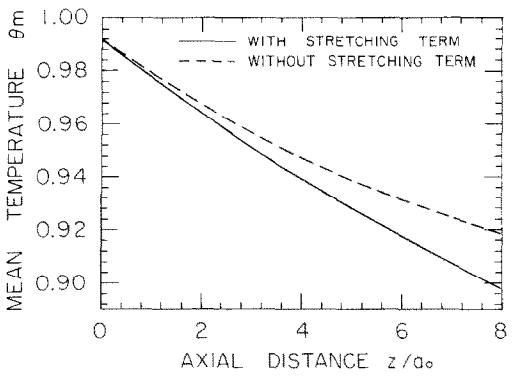

FIG. 7. Influence of stretching on the mixed mean temperatures.

number, *Re*, are based on the radius and the axial velocity. This formula was deduced from heat loss measurements on thin heated wires subjected to parallel air streams. Although the flow conditions of experiment P2 are beyond the Reynolds' number range of the correlation, its comparison to predictions based on boundary layer theory is informative since the formula is used widely in the analysis of fiber drawing flows. For the flow conditions of Fig. 6, the Kase and Matsuo formula predicts Nusselt numbers 35–70% lower than those predicted from the boundary layer theory that includes the stretching effect.

A finite element analysis was performed for the flow conditions of Krishnan's experiment P1. From Table 1, it can be seen that the mass flow rate is larger and the end radius is smaller for this case than for case P2. This implies that more drawing force had to be applied to the take-up of this jet to achieve the larger attenuation of the radius. A larger tension in the jet means a larger axial strain rate, which results in more viscous dissipation in the jet. The Brinkman number based on the flow conditions at the tube exit, is $Br \cong 10^{-4}$. However, it increases very rapidly becoming $\Theta(1)$ six radii downstream from the exit. Therefore, dissipation in the jet is very significant for the flow conditions of experiment P1. The Brinkman number was an order of magnitude smaller for the flow conditions of experiment P2. Attempts to model the flow conditions of experiment P1 were not successful. It was not possible to obtain a temperature field in the jet that continuously decreased in the streamwise direction when the jet was drawn down to the end radius reported in the experimental results. Figure 9 shows the mixed mean temperature of the jet derived from the finite element solution. The curve labeled 'run-away case (a)' corresponds to the attempt to draw the jet down to the end radius reported in the experimental results. A contour plot of the temperature field in the fiber is shown in Fig. 3(a). It should be noted that the finite element solution converged numerically. However, attempts to extend the solution in the axial direction using the small slope theory equations resulted in a velocity field that quickly diverged. In other words the force imposed on the end cut does not correspond to a valid operating condition of steady flow of the whole jet. Thus the term 'run-away' implies non-existence of steady flow under the assumed boundary conditions. A run-away situation can be thought of as follows. From the small slope theory, the viscous tension in the jet for a Newtonian fluid is

$$F = \frac{3\mu Q}{w}\frac{dw}{dz}. \tag{15}$$

For jet flows of highly viscous materials, such as Arochlor, the tension in the jet is essentially constant (independent of z). If the above equation is rearranged, the axial strain rate in the jet is

$$\frac{dw}{dz} = \frac{wF}{3\mu Q}. \tag{16}$$

The axial strain rate is thus inversely proportional to the viscosity. For a flow in which the tension in the jet is constant, and the temperature has begun to increase in the streamwise direction, the axial strain rate will increase as the viscosity decreases. However, this will increase the dissipation rate which only exacerbates the situation. Thus, if other conditions are fixed, a maximum draw force exists in the space of steady flow operating conditions. Beyond this value a numerical solution will deteriorate or 'run-away'.

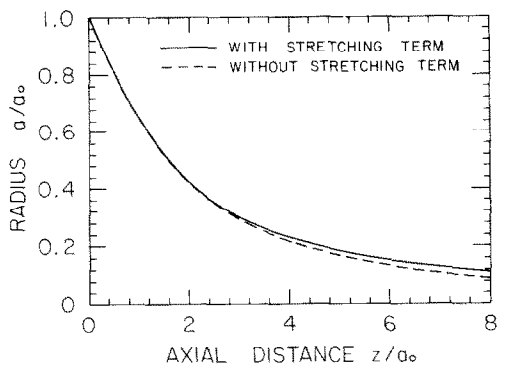

FIG. 8. Influence of stretching on the free surface shape of the fiber.

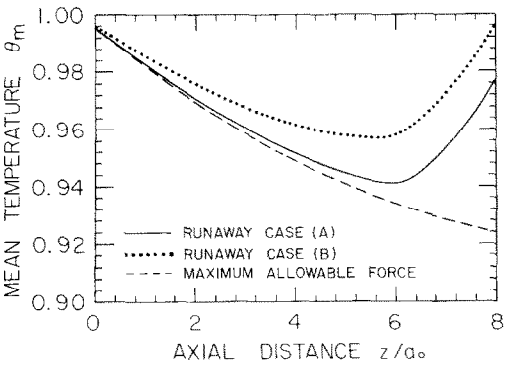

FIG. 9. Mixed-mean temperature distributions from the finite element modeling of Krishnan's flow P1.

The curve shown in Fig. 9, labeled 'maximum allowable force', shows the mixed mean temperature of the jet when the force applied to the end was relaxed to a point such that a continuously decreasing temperature distribution resulted. Figure 10 shows the shapes of the jets for these two situations. The drawing forces applied to the ends of these jets were: $F = 12\,452$ and $11\,156$ dyn for the run-away and the maximum allowable force, respectively. A 10% reduction of the end force eliminated the run-away situation, but the end radius increased by 63%. The run-away situation can be fully appreciated from the earlier work of Ben-Sabar [12], who omitted dissipation from his finite element analysis of experiment P1. The difference is drastic since the end force then becomes arbitrarily adjustable, and the predicted free surface can thereby be brought into correspondence with the experimental one.

A finite element solution for the flow conditions of experiment P1 was also obtained using the rigid cylinder boundary layer theory for the calculation of convective heat transfer. The run-away was slightly more severe since the heat transfer from the jet to the surroundings was less when the stretching effect was omitted from the analysis of the boundary layer. In Fig. 9 the curve labeled 'run-away case (b)' corresponds to this solution.

It appears that Krishnan created a flow situation very close to an actual run-away case. As previously mentioned, Krishnan found that the tensile force applied to the ends of the jets could not be too large otherwise the fibers would break during drawing. The failure of the heat transfer model to predict a stable flow for these conditions can be attributed to several factors. Radiation heat losses could have some influence on the solution. Also, since the jet is very thin, any cross-flowing air currents present during the experiment could also influence the cooling of the jet. Some attempts were made to perturb various flow parameters within a reasonable range of experimental error (5–20%) to find out if the maximum allowable force could be increased so that the predicted free surface shape coincided with the experimental one. However, these attempts were unsuccessful, and it appears that the discrepancy can be resolved only with an improved model of the surface heat loss mechanism.

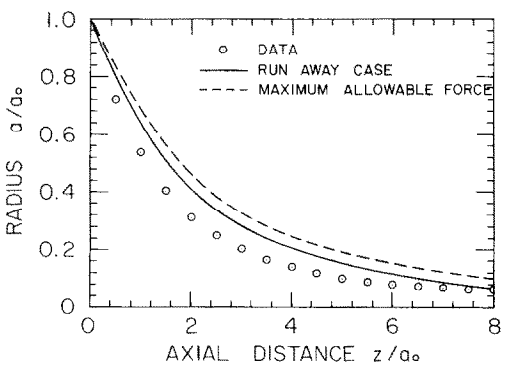

FIG. 10. Free surface shapes from the finite element solutions compared to Krishnan's data for the flow P1.

CONCLUSIONS

A finite element analysis of the convection cooling of the upper jet regions of fiber drawing flows has been presented in this paper. The problem is characterized by fully 2-D fields and complexities such as viscous dissipation, temperature-dependent viscosity, inertia, gravity, and surface tension forces. The viscous air drag was calculated using a boundary layer theory which accounts for the stretching jet surface. Reynolds' analogy was assumed for the calculation of the convective heat transfer coefficients. It was shown that neglecting the stretching of the jet surface in the analysis of the boundary layer (rigid cylinder theory) may lead to an appreciable difference in the calculated heat transfer coefficients. Also, this difference can significantly alter the development of the jet if the viscosity of the jet fluid is temperature-dependent.

The Nusselt numbers calculated from the boundary layer theory that includes the effect of stretching were compared to those calculated from the empirical formula of Kase and Matsuo [21]. Their formula predicted Nusselt values 35–70% smaller than those predicted from the boundary layer theory. This comparison is of interest since their formula has found considerable application [21–23].

In isothermal flows, the normal stress on a cross-section is uniform in the 1-D flow region since the viscosity of the jet fluid is everywhere constant, and the axial strain rate in the jet is independent of r. For nonisothermal flows in which the viscosity of the jet fluid is temperature-dependent, the distribution of normal stress on a cross-section is not uniform since there is a fully 2-D temperature field present. In this analysis the distribution of normal stress applied to the end of the jet was assumed to be proportional to the local viscosity multiplied by the axial strain rate. This assumption is consistent with the small slope theory conclusion that the axial strain rate is independent of r. Typical stresses calculated from the finite element solutions show less than 1% deviation from those applied to the end of the jet.

The convective heat transfer model was used to analyze the flow conditions reported in the experimental results of Krishnan [2]. Krishnan reported jet shapes for two sets of flow conditions. The free surface shape of the jet was predicted quite well for one set of flow conditions where viscous dissipation was not very significant. In this case it was possible to adjust the end force such that the predicted free surface shape coincided with the experimental result. For the other set of flow conditions, the viscous dissipation was more pronounced and the heat transfer model was not capable of predicting a continuously decreasing temperature distribution in the jet. In this case it was not possible to adjust the end force to obtain a suitable free surface shape and, therefore, this case can be

considered to be a critical test of the heat transfer model. This point becomes even clearer from the work of Ben-Sabar [12] who simulated this flow leaving out the dissipation terms. He was able to adjust the end force to obtain a prediction of the free surface in excellent agreement with Krishnan's data. The heat transfer model presented in this paper allowed a larger end force to be applied to the jet than previous models. However, the failure of the present model to predict a continuously decreasing temperature field in the jet indicates that further research of both the heat loss mechanism and the drawing of fibers of temperature-sensitive materials is warranted. The curve fitting power gained from the use of the force as an adjustable parameter implies that experiments of this kind are needed in which the test fluid is completely characterized, and a complete set of operating conditions are measured. This means that temperatures along the developing jet need to be measured, and that force measurements should be made close to the region to be stimulated. These requirements present formidable experimental difficulties.

REFERENCES

1. L. R. Glicksman, The dynamics of a heated free jet of variable viscosity liquid at low Reynolds numbers, *J. Basic Engng* **90,** 343–354 (1968).
2. S. Krishnan, Dynamics of a heated jet, M.S. thesis, Massachusetts Institute of Technology, Cambridge, Massachusetts (1969).
3. R. E. Sayles, A finite element analysis of the upper jet region of a fiber drawing flow field, Ph.D. thesis, Brown University, Providence, Rhode Island (1981).
4. B. C. Sakiadis, The boundary layer on a continuous cylindrical surface, *A.I.Ch.E. Jl* **7,** 467 (1961).
5. B. A. Finlayson, *The Method of Weighted Residuals and Variational Principals.* Academic Press, New York (1972).
6. K. H. Huebner, *The Finite Element Method for Engineers,* Wiley, New York (1975).
7. C. C. Zienkiewicz, *The Finite Element Method in Engineering Science.* McGraw-Hill, London (1971).
8. R. E. Nickell, R. I. Tanner and B. Caswell, The solution of viscous incompressible jet and free surface flows using finite element methods, *J. Fluid Mech.* **65,** 189–206 (1974).
9. E. Ben-Sabar and B. Caswell, A stable finite element simulation of convective transport, *Int. J. Numerical Methods* **14,** 545–565 (1979).
10. A. R. Faiz, An investigation of low Reynolds number free vertical jet flows, Ph.D. thesis, University of Rhode Island, Kingston, Rhode Island (1978).
11. R. J. Fisher, M. M. Denn and R. I. Tanner, Initial profile development in melt spinning, *Ind. Engng Chem. Fundam.* **19,** 195–197 (1980).
12. E. Ben-Sabar, A finite element analysis of the non-isothermal jet flow in the fiber spinning process, Ph.D. thesis, Brown University, Providence, Rhode Island (1980).
13. L. Rongved, Stress in glass fibers induced by the draw force, *J. Appl. Mech.* **45,** 765–772 (1978).
14. D. E. Bourne and D. G. Elliston, Heat transfer through the axially symmetric boundary layer on a moving circular fibre, *Int. J. Heat Mass Transfer* **13,** 583 (1970).
15. D. E. Bourne and H. Dixon, The cooling of fibers in the formation process, *Int. J. Heat Mass Transfer* **24,** 1323 (1971).
16. M. B. Glauert and M. J. Lighthill, The axisymmetric boundary layer on a long thin cylinder, *Proc. R. Soc.* **230A,** 188–203 (1955).
17. W. Jou, Boundary layer development and heat transfer for fiber spinning, paper presented at the Proceedings of the 1978 Heat Transfer and Fluid Mechanics Institute, Pullman, Washington, June (1978).
18. C. A. Moore and J. R. A. Pearson, Experimental investigations into an isothermal spinning threadline: extensional rheology of a separan AP 30 solution in glycerol and water, *Rheol. Acta* **14,** 436–446 (1975).
19. E. M. Sparrow, R. Eichhorn and J. L. Gregg, Combined forced and free convection in a boundary layer flow, *Physics Fluids* **2**(3), 319–328 (1959).
20. T. R. Barnett, Calculation of the temperature of filaments in melt spinning, *Appl. Polymer Symp.* No. 6, 51–65 (1967).
21. S. Kase and T. Matsuo, Studies on melt spinning, I. Fundamental equations on the dynamics of melt spinning, *J. Polymer Sci.* **3,** 2541–2554 (1965).
22. R. J. Fisher and M. M. Denn, Mechanics of nonisothermal polymer melt spinning, *A.I.Ch.E. Jl* **23**(1), 23–38 (1977).
23. Y. Shah and J. R. A. Pearson, On the stability of nonisothermal fiber spinning, *Ind. Engng Chem. Fundam.* **11**(2), 145–149 (1972).

UNE ANALYSE PAR ELEMENTS FINIS DE LA REGION SUPERIEURE D'UN JET DE FIBRE POUR UN MATERIAU SENSIBLE A LA TEMPERATURE

Résumé—La méthode des éléments finis est appliquée à l'analyse du refroidissement convectif de la région supérieure d'un écoulement de fibre. Cette région est caractérisée par des champs de vitesse et de température pleinement bidimensionnels, l'apparence d'une surface libre et une forte atténuation du rayon du jet. Le transfert thermique convectif sur le jet est calculé en utilisant une théorie de couche limite dans laquelle l'effet de déploiement de la surface du jet est pris en compte et l'analogie de Reynolds est admise pour le calcul des coefficients de convection. On modélise des écoulements de jets pour l'Arochlor, matériau très sensible à la température. Les formes de la surface libre calculées à partir du modèle sont comparées à celles obtenues expérimentalement. On trouve que le degré de précision dans le calcul de la forme de la surface libre du jet dépend fortement de l'importance de la dissipation visqueuse dans l'écoulement.

EINE RECHNERISCHE UNTERSUCHUNG DES FASERSPINNSTRÖMUNGSFELDES EINES TEMPERATUREMPFINDLICHEN MATERIALS IM OBEREN DÜSENBEREICH MIT HILFE FINITER ELEMENTE

Zusammenfassung—Die Methode der finiten Elemente wurde in einer Analyse der konvektiven Abkühlung des oberen Bereichs einer Faserströmung angewandt. Dieses Gebiet ist durch ausgesprochen zweidimensionale Geschwindigkeits- und Temperaturfelder, das Auftreten einer freien Oberfläche und die starke Abnahme des Strahlradius gekennzeichnet. Der konvektive Wärmeübergang am Strahl wird unter Verwendung einer Grenzschichttheorie berechnet, die den Einfluß der sich ausdehnenden Strahloberfläche berücksichtigt. Zur Berechnung der konvektiven Wärmeübergangskoeffizienten wurde Gültigkeit der Reynolds-Analogie angenommen. Die Strahlströmung des sehr temperaturempfindlichen Stoffes Arochlor wurde simuliert. Die mit dem Modell der finiten Elemente berechnete Form der freien Oberfläche des Strahls wurde mit experimentell ermittelten Strahlformen verglichen. Die Genauigkeit, mit der die Form der freien Strahloberfläche mit Hilfe der finiten Elementen-Methode vorausberechnet werden kann, hängt stark vom Reibungsverlustanteil innerhalb des Strahls ab.

ИСПОЛЬЗОВАНИЕ МЕТОДА КОНЕЧНЫХ ЭЛЕМЕНТОВ ДЛЯ АНАЛИЗА СТРУИ В ВЕРХНЕЙ ЕЕ ЧАСТИ ПРИ ВЫТЯЖКЕ ВОЛОКНА ИЗ ТЕРМОЧУВСТВИТЕЛЬНОГО МАТЕРИАЛА

Аннотация—Для анализа конвективного охлаждения верхней области струи при вытяжке волокна использован метод конечных элементов. Эта область течения характеризуется двумерными полями скорости и температуры, наличием свободной поверхности и значительным уменьшением радиуса струи. Конвективный теплоперенос от струи рассчитывается с помощью теории пограничного слоя, в которой учитывается эффект растяжения поверхности струи, а для расчета коэффициентов конвективного теплопереноса предполагается справедливость аналогии Рейнольдса. Моделировались струйные течения арохлора – материала с высокой степенью термочувствительности. Формы свободной поверхности струй, рассчитанные по модели конечных элементов, сравнивались с формами, полученными экспериментальным путем. Найдено, что степень точности, с которой может быть рассчитана форма свободной поверхности струи с помощью модели конечных элементов, сильно зависит от вязкой диссипации струйного течения.